THE JOURNAL OF PHYSICAL CHEMISTRY B

Article

pubs.acs.org/JPCB

Multifrequency EPR Study of Fe^{3+} and Co^{2+} in the Active Site of Desulforedoxin

Guinevere Mathies,[†] Rui M. Almeida,[‡] Peter Gast,[†] José J. G. Moura,[‡] and Edgar J. J. Groenen[†,*]

[†]Department of Physics, Huygens Laboratory, Leiden University, The Netherlands

[‡]REQUIMTE/CQFB, Departamento de Química, Faculdade de Ciências e Tecnologia, Universidade Nova de Lisboa, Lisbon, Portugal

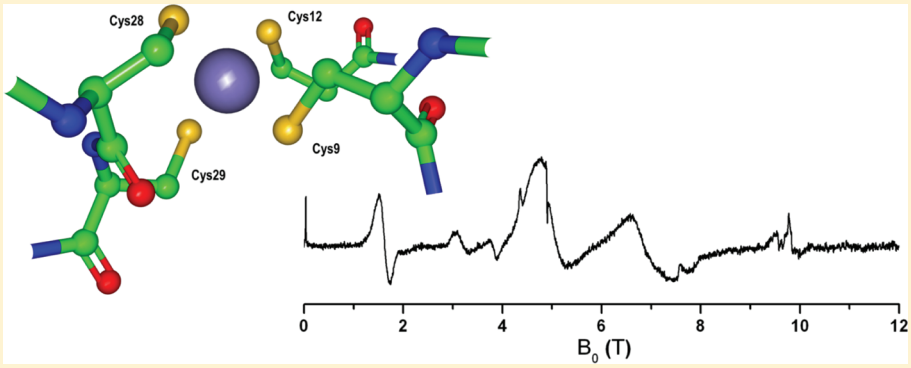

ABSTRACT: The understanding of the electronic structure of $S > 1/2$ transition-metal sites that show a large zero-field splitting (ZFS) of the magnetic sublevels benefits greatly from study by electron-paramagnetic-resonance (EPR) spectroscopy at frequencies above the standard 9.5 GHz. However, high-frequency EPR spectroscopy is technically challenging and still developing. Particularly the sensitivity of high-frequency EPR spectrometers is often too low to apply the technique in the study of transition-metal sites in proteins and enzymes. Here we report a multifrequency EPR study (at 9.5, 94.9, and 275.7 GHz) of the active site of the protein desulforedoxin, both in its natural Fe^{3+} form and substituted with Co^{2+}. The 275.7 GHz EPR spectra made it possible to determine the ZFS parameters of the Fe^{3+} site with high precision. No 275.7 GHz spectrum could be observed of the Co^{2+} site, but based on 9.5 GHz spectra, its ZFS parameters could be estimated. We find that the typical variation in the geometry of the active site of a protein or enzyme, referred to as conformational strain, does not only make the detection of EPR spectra challenging, but also their analysis. Comparison of the EPR results on the active site of desulforedoxin to those of the closely related active site of rubredoxin illustrates the necessity of explicit quantum-chemical calculations in order to interrelate the electronic and geometric structure of biological transition-metal sites.

INTRODUCTION

In many proteins and enzymes, the active site contains a paramagnetic transition-metal ion and electron-paramagnetic-resonance (EPR) spectroscopy can provide detailed information on its electronic structure. This makes EPR spectroscopy an invaluable tool in the study of the relationship between structure and function of the active sites in biological molecules.[1−3] Whenever the transition-metal ions carry a spin angular momentum $S > 1/2$ the degeneracy of the magnetic sublevels may already (partly) be lifted in the absence of an external magnetic field. For such systems it is advantageous, or even required, to record EPR spectra at a microwave frequency comparable to or larger than this zero-field splitting (ZFS), and one needs an EPR spectrometer operating at a frequency higher than the standard 9.5 GHz (X band). Fortunately, the last decades have shown a strong increase in the possibilities to perform EPR spectroscopy at higher frequencies.

An EPR spectrum is to be analyzed in terms of its spin-Hamiltonian parameters, which then have to be translated into electronic structure using advanced quantum-chemical methods. Considerable progress has been made with such calculations in recent years, in particular based on density-functional theory, but calculation of the ZFS for transition-metal ions remains still in an exploratory stage,[4] particularly for biological sites. Consequently there is a need for more experimental data on such systems that can be used as benchmarks.

A challenge in high-frequency EPR is to achieve the sensitivity needed to study transition-metal sites in biological molecules. Recently we have demonstrated that, using a single-mode cavity, it is possible to record high-quality EPR spectra in continuous-wave (cw) mode at 275.7 GHz (J band) of mM frozen solutions of the protein rubredoxin, whose active site in the oxidized state contains high-spin Fe^{3+}.[5] We were able to

Received: March 16, 2012
Revised: May 12, 2012
Published: May 21, 2012

dx.doi.org/10.1021/jp3025655 | J. Phys. Chem. B 2012, 116, 7122−7128

detect differences on the order of 1 GHz in the ZFS between rubredoxins from different organisms. Here we study the closely related active site of the protein desulforedoxin by multifrequency EPR, both in its natural high-spin Fe^{3+} ($S = {}^5/_2$) form and substituted with high-spin Co^{2+} ($S = {}^3/_2$).

The rubredoxin class of small proteins found in sulfur-metabolizing bacteria and archaea is known to participate in electron transport.[6] The rubredoxin active site comprises an iron atom bound in an approximately tetrahedral geometry to four cysteine residues, which occur in two ...x-Cys-x-x-Cys-Gly-x... segments. Desulforedoxin is a homodimer consisting of two, 36 amino acid chains[7,8] and has two equivalent $Fe(S\text{-}Cys)_4$ active sites. The site geometry is again approximately tetrahedral, but the four cysteine residues occur in an ...x-Cys-x-x-Cys-Gly-x... and an ...x-Cys-Cys-Gly-x... segment.[9]

High-spin Fe^{3+} in a four-sulfur coordination has been studied both theoretically[10−12] and experimentally by several spectroscopic methods, both in model complexes,[13−16] and in rubredoxin.[17−19] High-spin Co^{2+} in a four-sulfur coordination has been studied to a lesser extent.[20−24] Cobalt does not occur as frequently in biological molecules as iron; yet it is a rewarding spectroscopic probe, for instance as a substitute for diamagnetic Zn^{2+}.[25] In the case of desulforedoxin the substitution of Fe^{3+} by Co^{2+} constituted an interesting opportunity to study biological CoS_4 coordination.

Desulforedoxin has been investigated by Moura et al. by X-band EPR and by Mössbauer spectroscopy.[18,26,27] Moura et al. also recorded an X-band spectrum of Co(II)-substituted desulforedoxin.[28]

We report cw EPR spectra of a frozen solution of Fe(III)-desulforedoxin at J band and X band. The J-band spectra make it possible to determine the ZFS parameters accurately and reveal a small g-anisotropy. No J-band spectrum could be observed of Co(II)-substituted desulforedoxin. The X-band spectra of a frozen solution of Co(II)-desulforedoxin at multiple temperatures allow an estimate of the spin-Hamiltonian parameters. The typical variation in the geometry of the active site of a protein or enzyme, referred to as conformational strain, does not only make the detection of their EPR spectra challenging, but also complicates the analysis. The differences between the ZFS parameters of the high-spin Fe^{3+} site of desulforedoxin, the high-spin Fe^{3+} site of rubredoxin and the high-spin Co^{2+} substituted site of desulforedoxin are discussed.

MATERIALS AND METHODS

Desulforedoxin from *Desulfovibrio gigas* was expressed in *Escherichia coli* and purified following a procedure similar to the procedure described in ref 29 for rubredoxin. Reconstitution with Co^{2+} was performed as described in ref 28. All proteins were kept in 20 mM Tris buffer at pH 7.6. Samples for X-band EPR contained 20% glycerol.

The cw J-band EPR spectra were recorded on an in-house developed spectrometer,[30] using a probe head specialized for operation in cw mode as described in reference5. The effective sample volume, limited by the microwave cavity, is approximately 20 nL. The cw W-band (94.1 GHz) spectra were recorded on a Bruker Elexsys E680 spectrometer using a W-band "ENDOR" probe head with a cylindrical TE_{011} cavity in a CF935W flow cryostat (Oxford Instruments). Pulsed W-band (94.9 GHz) spectra were recorded on an in-house developed spectrometer.[31] The cw X-band spectra were also recorded on a Bruker Elexsys E680 spectrometer, using a TE_{102} rectangular cavity equipped with an ESR 900 Cryostat (Oxford Instruments).

RESULTS AND ANALYSIS

Desulforedoxin. Figure 1 shows cw J-band spectra of a frozen solution of desulforedoxin at 5 and 25 K. The complex

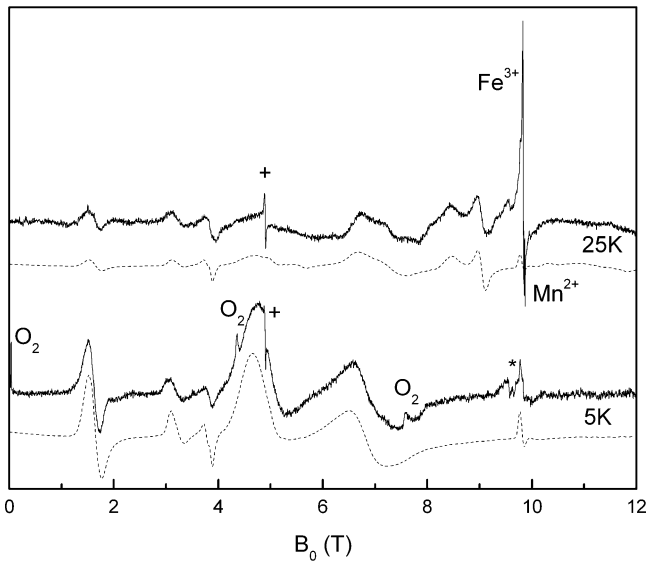

Figure 1. J-band cw EPR spectra of a 10 mM frozen solution of desulforedoxin from *D. gigas* at 5 and 25 K. Experimental conditions: modulation amplitude: 3 mT, microwave power: 1 μW, microwave frequency: 275.7 GHz. Solid lines: experimental spectra. Dashed lines: spectra calculated using EasySpin and the spin-Hamiltonian parameters given in the text. Experimental spectra are smoothed by adjacent averaging and are baseline corrected at the low- and high-field end. An unknown impurity in the cavity gives a negative peak at 9.6 T, marked with an asterisk. The following background signals arise from the frozen solution. At both temperatures a narrow transition at 4.9 T, marked with a plus sign, is due to an unknown impurity. In the 5 K spectrum signals due to oxygen are observed.[32] At 25 K, the strong transition around $g = 2$ (9.84 T), which has a shoulder on the low-field side, is due to an unknown rhombic high-spin Fe^{3+} contaminant and a detailed scan of the $g = 2$ region revealed six lines of Mn^{2+}.

spectrum covers a field range of more than 10 T. The 5 K spectrum shows three signals that lose intensity at elevated temperatures at 1.7 T and around 4.7 and 6.5 T. These last two signals have a width of almost 1 T. In the 25 K spectrum signals appear around 7.0, 8.4, and 9.0 T.

Figure 2 shows cw X-band spectra of a frozen solution of desulforedoxin at 5, 10, and 80 K. In the spectra three signals, at 86.6, 162, and 369 mT, lose intensity as temperature increases. The signals at 162 and 369 mT are considerably broader than the signal at 86.6 mT. A signal at 116.4 mT remains relatively strong at elevated temperatures.

The following spin Hamiltonian is used to interpret the EPR spectra arising from high-spin Fe^{3+}, $S = {}^5/_2$.[33]

$$H = \mu_B \vec{B}_0 \cdot \overrightarrow{g} \cdot \vec{S} + \vec{S} \cdot \overrightarrow{D} \cdot \vec{S} \qquad (1)$$

The first term describes the electron Zeeman interaction. A first-order contribution from spin−orbit coupling induces g-anisotropy, but this anisotropy is expected to be small, since high-spin Fe^{3+} has an S ground state. The second term describes the ZFS, which splits the six magnetic sublevels into

dx.doi.org/10.1021/jp3025655 | J. Phys. Chem. B 2012, 116, 7122−7128

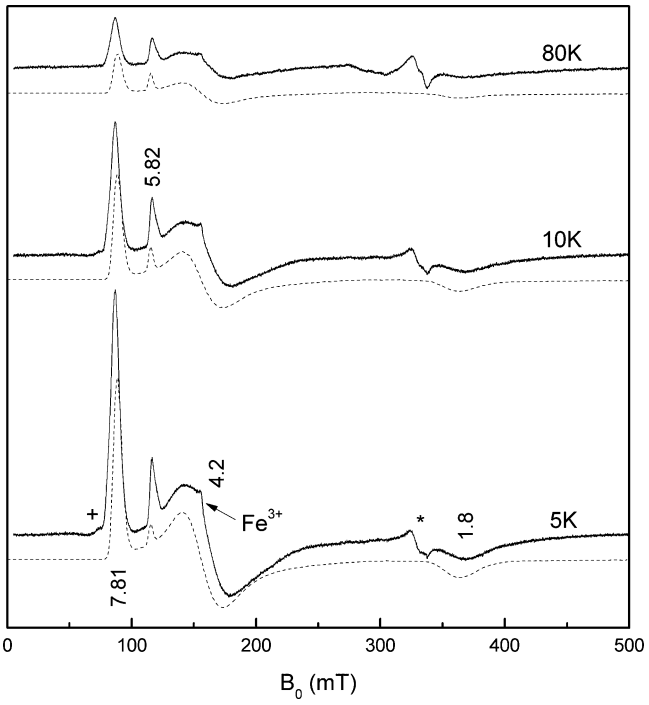

Figure 2. X-band cw EPR spectra of a 0.6 mM frozen solution of desulforedoxin from *D. gigas* at 5, 10, and 80 K. Experimental conditions: modulation amplitude, 1 mT; microwave power, 5 and 10 K spectra, 1.3 mW, and 80 K spectrum, 20 mW; microwave frequency, 9.491 GHz. Solid lines: experimental spectra. Dashed lines: spectra calculated using EasySpin and the spin Hamiltonian parameters determined from the J-band spectra. The *g*-values of the resonances from desulforedoxin are shown in the graph. The signal marked with an asterisk just below $g = 2$ (331 mT) is due to an impurity in the cavity. The signal marked with a plus sign is an unknown impurity in the frozen solution, which was also observed by Moura et al.,[18,26] and the signal around $g = 4.3$ (157 mT) is due to an unknown rhombic high-spin Fe^{3+} contaminant.

three Kramers doublets. The ZFS-tensor, $\vec{\vec{D}}$, is symmetric, can be taken traceless, and is characterized by two parameters, D and E.

$$D = 3/2D_z,\ E = 1/2(D_x - D_y) \qquad (2)$$

The rhombicity of $\vec{\vec{D}}$ is given by the ratio $\lambda = E/D$. The principal axes are chosen such that $|D_z| > |D_y| > |D_x|$ and $0 < \lambda < 1/3$.

From X-band EPR and Mössbauer spectra of desulforedoxin, Moura et al. estimated λ to be 0.08 and D to be 2 cm^{-1} or 60 GHz,[18,26,33] which explains the complexity of the desulforedoxin spectra in Figure 1. In the magnetic field range where the J band resonances occur the two terms in the spin Hamiltonian are comparable in size and the three Kramers doublets are intertwined. Analysis of the J-band spectra was performed by comparison to spectra calculated by numerical diagonalization of the spin Hamiltonian using the EPR simulation package EasySpin,[35] taking the parameters of Moura et al. as a starting point. The principal axes of the *g*-tensor are assumed to be collinear with those of the *D*-tensor. The experimental J-band spectra were best reproduced taking $D = 72$ GHz and $\lambda = 0.074$. Increasing the principal values of the *g*-tensor to above the free electron value improved the simulation: g_x, $g_y = 2.020$, $g_z = 2.025$. To reproduce the width and shape of the resonances in the J-band spectra a strain in D and E of 20% was taken into account using a first-order approximation (see the online documentation on EasySpin); cf. Discussion.

At X band the ZFS is larger than the microwave quantum of 9.5 GHz and only intradoublet transitions can be observed. The system approaches the regime where each of the three Kramers doublets can be approximated as an effective $S' = {}^1/_2$ system.[36] In this regime the anisotropic Zeeman splitting of each doublet is reflected in effective *g*′-values, g_x', g_y', and g_z', which depend on the *g*-values and λ, but not on D. The signals at the effective *g*′-values of 7.81, 4.2 and 1.8, which lose intensity at elevated temperatures, arise from the lowest doublet, $\pm{}^1/_2$. The signal at $g' = 5.82$ is found to arise from the middle $\pm{}^3/_2$-doublet. The dashed lines in Figure 2 are spectra calculated using the parameters determined from the J-band spectra. In these spectra the line broadening was simulated by using a Gaussian distribution in λ of fwhm = 0.035, which corresponds to a distribution width of approximately 20% in D and E. The experimental spectra are reproduced, but there are small differences, on the order of 1 mT, between the calculated and experimental fields of resonance.

Co(II)−Desulforedoxin. Figure 3 shows cw X-band spectra of a frozen solution of Co(II)-desulforedoxin at 5, 10, 25, and

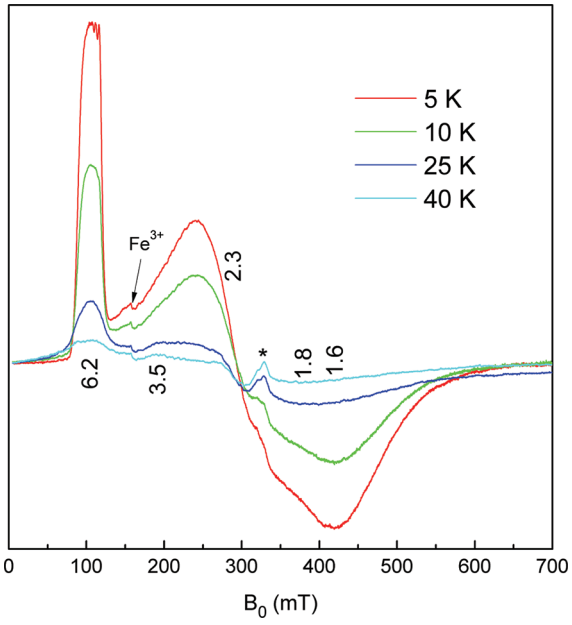

Figure 3. X-band cw EPR spectra of a 0.7 mM frozen solution of Co(II)-desulforedoxin from *D. gigas* at 5, 10, 25, and 40 K. Experimental conditions: modulation amplitude, 1.5 mT; microwave power, 200 mW; microwave frequency, 9.495 GHz. A baseline was subtracted. The *g*-values of the resonances from desulforedoxin are shown in the graph. The signal marked with an asterisk around $g = 2$ (331 mT) is due to an impurity in the cavity. The signal around $g = 4.3$ (157 mT) is due to an unknown rhombic high-spin Fe^{3+} contaminant.

40 K. At 5 K three transitions can be observed, around 110, 290, and 420 mT. The middle- and high-field transitions are very broad and overlap. Upon increase of the temperature these three transitions lose intensity. At 25 and 40 K a new transition can be observed around 192 mT. The minimum found at low temperature around 420 mT shifts to around 380 mT at elevated temperatures. The transition around 110 mT preserves some of its intensity at 40 K and broadens.

dx.doi.org/10.1021/jp3025655 | J. Phys. Chem. B 2012, 116, 7122−7128

At J band no spectrum of Co(II)−desulforedoxin could be detected. At W band an electron-spin−echo (ESE) detected EPR spectrum was observed at 1.7 K, shown in Figure 4. A spin

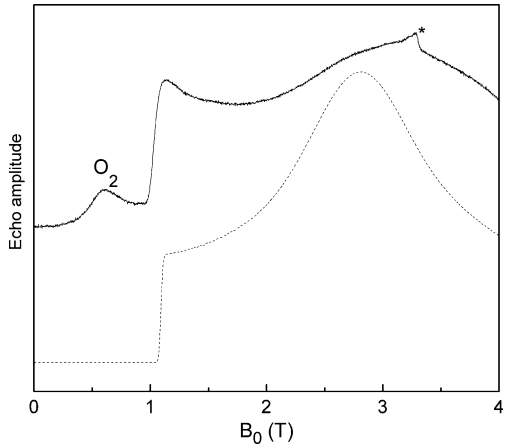

Figure 4. W-band ESE-detected EPR spectra of a 0.7 mM frozen solution of Co(II)-desulforedoxin from *D. gigas* at 1.7 K. Experimental conditions: a two-pulse Hahn echo is generated by the pulse sequence $\pi/2-\tau-\pi$ = 70−405−140 ns; repetition time, 1 ms; microwave power, 1 mW; microwave frequency, 94.9 GHz. Solid line: experimental spectrum. Dashed line: spectrum calculated using EasySpin and the spin-Hamiltonian parameters given in the text. The signal around 0.6 T results from oxygen in the frozen solution.[32] The signal marked with an asterisk at g = 2 (3.39 T) results from an unknown impurity.

echo due to Co(II)-desulforedoxin was detected at magnetic fields above 1.1 T. The echo amplitude reached a maximum around 3.2 T. An attempt was made to measure the cw spectrum of a 4 mM frozen solution of Co(II)−desulforedoxin at W band. At 6.5 K a peak around 1 T showed up very weakly.

To interpret the high-spin Co^{2+}, $S = {}^3/_2$, spectra a term describing the hyperfine interaction with the ^{59}Co nucleus ($I = {}^7/_2$) should be added to the spin Hamiltonian eq 1.

$$H = \mu_B \vec{B}_0 \cdot \overrightarrow{\vec{g}} \cdot \vec{S} + \vec{S} \cdot \overrightarrow{\vec{D}} \cdot \vec{S} + \vec{S} \cdot \overrightarrow{\vec{A}} \cdot \vec{I} \quad (3)$$

The ground state of high-spin Co^{2+} is an F state. A first-order contribution from spin−orbit coupling induces considerable g-anisotropy. The ZFS, which is large, typically hundreds of GHz, splits the four energy levels of the ground state into two Kramers doublets. The contribution of a nuclear Zeeman interaction by cobalt can be neglected.

Analysis of the X-band spectra is performed under the assumption that the effective $S' = {}^1/_2$ description of the doublets is valid. For an $S = {}^3/_2$ system the effective g_i'-values are related to the g_i-values by[36−38]

$$g_x' = g_x\left(1 \pm \frac{1-3\lambda}{\sqrt{1+3\lambda^2}}\right)$$

$$g_y' = g_y\left(\pm 1 + \frac{1+3\lambda}{\sqrt{1+3\lambda^2}}\right)$$

$$g_z' = g_z\left(\mp 1 + \frac{2}{\sqrt{1+3\lambda^2}}\right) \quad (4)$$

The upper signs refer to the $\pm{}^1/_2$ doublet and the lower signs to the $\pm{}^3/_2$ doublet. Note that these relations presume that the principal axes of the g- and D-tensor are collinear.

The transitions observed in the 5 K spectrum, at effective g'-values 6.2, 2.3, and 1.6 respectively, are due to the anisotropic splitting of the lower Kramers doublet. At 25 and 40 K the spectra are dominated by three transitions at effective g'-values 6.2 (110 mT), 3.5 (192 mT) and 1.8 (380 mT), which arise from the upper Kramers doublet. Following Equation eq 4, the transition at $g' = 3.5$ must be the g_x' transition of the $\pm{}^1/_2$ doublet. Hence, the $\pm{}^1/_2$ doublet is higher in energy and D is negative. Equation eq 4 and a minimization procedure were used to estimate the values of λ and g_x, g_y, and g_z from the six observed effective g'-values. This gave $\lambda = 0.26$, $g_x = 2.9$, $g_y = 2.4$, and $g_z = 2.2$. These values are, together with a large, negative D, used to simulate the Co(II)−desulforedoxin spectra with EasySpin,[34] as shown for the 5 K spectrum in Figure 5. The shape of the experimental spectra is qualitatively reproduced by the simulation, but fine-tuning is clearly needed. This has not been pursued, see Discussion.

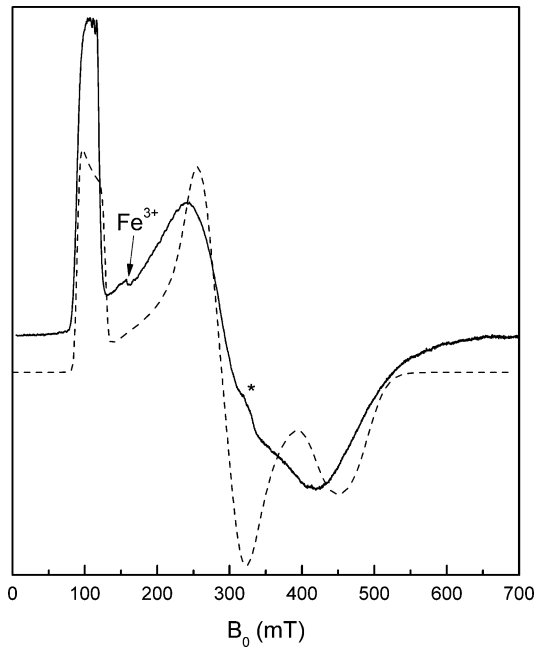

Figure 5. X-band cw EPR spectrum of a 0.7 mM frozen solution of Co(II)-desulforedoxin from *D. gigas* at 5 K. Solid line: experimental spectrum. Dashed line: spectrum calculated using EasySpin and the spin-Hamiltonian parameters given in the text. The signal marked with an asterisk around g = 2 (331 mT) is due to an impurity in the cavity. The signal around g = 4.3 (157 mT) is due to an unknown rhombic high-spin Fe^{3+} contaminant.

To simulate line broadening in the X-band spectra, a Gaussian distribution in λ of fwhm 0.035 was used. The broadening of the $g_z'(\pm{}^3/_2)$ transition is mainly due to a (partially resolved) hyperfine interaction with the ^{59}Co nucleus of approximately A_z = 150 MHz.

The dashed spectrum in Figure 4 is the absorption spectrum calculated using EasySpin and the spin-Hamiltonian parameters estimated from the frozen solution cw X-band spectra. It reproduces qualitatively the ESE detected EPR spectrum, i.e., the onset of the spin echo at 1.1 T, which corresponds to

dx.doi.org/10.1021/jp3025655 | J. Phys. Chem. B 2012, 116, 7122−7128

$g_z'(\pm^3/_2) = 6.2$, and the broad field range over which an echo is observed.

DISCUSSION

The cw J-band spectra of the frozen solution of desulforedoxin are well reproduced by spectra calculated from numerical diagonalization of the spin Hamiltonian,[35] see Figure 1, optimally with the ZFS parameters $D = 72 \pm 1$ GHz and $\lambda = 0.074 \pm 0.002$, and a small g-anisotropy, $g_x g_y = 2.020 \pm 0.001$, $g_z = 2.025 \pm 0.005$. The uncertainty in a parameter was estimated from the calculated shift of the J-band resonances upon a change in that parameter. Because the microwave quantum ($\nu = 275.7$ GHz) is larger than the ZFS, interdoublet transitions are possible and the spectrum is very sensitive to both E and D. An X-band spectrum, on the other hand, depends on $\lambda = E/D$, and D needs to be estimated via an elaborate temperature study.[17] Moreover, at X band the small g-anisotropy of high-spin Fe^{3+} is not resolved.

Conformational strain is typical for proteins and enzymes. The geometrical variations affect the electronic structure of active sites, which translates into a distribution in the ZFS parameters for high-spin Fe^{3+}[19,39] and in a distribution in the ZFS parameters and the principal values of the g-tensor for high-spin Co^{2+}. This does not only result in line broadening, which can make it difficult to detect the EPR spectrum of a biological site, but it may also deform the spectrum, which complicates its analysis. Particularly, if a change in a spin-Hamiltonian parameter results in a large change of the transition probability, strain can result in a shift of what appears to be the average field of resonance in the experimental EPR spectra.

In order to reproduce the line widths in the experimental J-band spectra of desulforedoxin, the spectra were simulated using EasySpin with a strain of about 20% in D and E. A first-order approximation is used, in which the spectrum was convoluted with a Gaussian of a width proportional to the derivative of the resonance field of a given transition with respect to, for instance, D; the proportionality constant is chosen by the user. This approximation is valid if the strain is much smaller than the parameter itself. In the high-field limit, $\mu_B \vec{B}_0 \cdot \vec{\vec{g}} \cdot \vec{S} \gg \vec{S} \cdot \vec{\vec{D}} \cdot \vec{S}$, where the magnetic field at which the resonances in a frozen solution spectrum are observed depends linearly on the principal values of the D-tensor,[40] the approximation may also be valid for larger strains in D and E, if the transition probability does not depend strongly on these parameters. This was found to be the case for Fe(III)-rubredoxin, $D = 48$ GHz, by comparison to spectra calculated using a distribution in D and E.[5] For desulforedoxin, $D = 72$ GHz, such a comparison was not feasible, because the calculation of the individual spectra is too time-consuming.

The X-band spectra of Fe(III)- and Co(II)-desulforedoxin are typical of a site that experiences large conformational strain: the resonances at low g-values are very broad, while the resonances at high g-values are narrower. The distributions in g_x', g_y', and g_z' are of similar width, but the distribution in the resonance fields will be broader for the smaller g_i'-values. To simulate the experimental X-band spectra of both sites, the effect of conformational strain was taken into account by using a Gaussian distribution in λ. For Fe(III)-desulforedoxin the experimental line width was well reproduced, but small deviations in the resonance fields remained between the experimental spectra and the calculated spectra when using the spin-Hamiltonian parameters determined from the J-band spectra. For Co(II)−desulforedoxin the line width is poorly reproduced and it is hard to say if the resonance fields are reproduced properly. Of course, a proper simulation of the Co(II)−desulforedoxin X-band spectra requires not only a distribution in λ, but also in g_x, g_y, and g_z.

For Co(II)−desulforedoxin not only the effect of conformational strain, but also the spin-Hamiltonian parameters are uncertain. The values of the parameters used in the simulation of the X-band spectra were merely an estimate. Following eq 4, the only possible assignment for the peak observed at $g' = 3.5$ at elevated temperatures is the g_x'-transition of the $\pm^1/_2$ doublet, making $D < 0$. However, the value of 2.9 for g_x, which has to be invoked to fit the observed $g_x'(\pm^1/_2) = 3.5$ and, particularly, the $g_x'(\pm^3/_2) = 2.3$ transition, is unusually large.[41,42] The quantitative analysis of the X-band spectrum of Co(II)-desulforedoxin is hampered by the very large ZFS in combination with a large g-anisotropy and the difficulties encountered when simulating the effects of conformational strain. A third complicating factor is that the principal axes of the D- and g-tensors may not be collinear due to the covalent character of the bonding with the soft sulfur ligands.[4,43,44] The relations in eq 4 are only valid if the principal axes of the D- and g-tensors are collinear and can therefore not be used in the analysis. Moreover, a reliable analysis by numerical diagonalization of the spin Hamiltonian is prohibited by the introduction of extra degrees of freedom due to the unknown relative orientation of the principal axes of the D- and g-tensors.

High-frequency EPR spectra of Co(II)−desulforedoxin could be helpful. First, they can provide information on the relative orientation of the principal axes of the D- and g-tensors. At X band the direction of the effective magnetic field is dominated by the D-tensor. If spectra are recorded at higher frequency and higher magnetic field, the influence of the Zeeman interaction on the direction of the effective magnetic field becomes noticeable. Also, at higher frequency deviations from the effective $S' = {}^1/_2$ picture start to occur, an effect that was used in the multifrequency EPR study of a high-spin Co^{2+} complex to estimate D.[24] Or, ideally, the regime $\nu \approx D$ is reached and interdoublet transitions become possible.[45−48]

Unfortunately no spectrum of Co(II)−desulforedoxin could be observed in cw at J-band. The ESE-detected W-band spectrum corroborates our interpretation of the cw X-band spectra, but fine-tuning of the parameters based on this spectrum is complicated by anisotropic relaxation times. No high-frequency studies of high-spin Co^{2+} in the active site of a protein are found in literature. The reason that high-frequency spectra of Co(II)-substituted desulforedoxin, and of biological high-spin Co^{2+} systems in general, are hard to come by is the large g-anisotropy. Conformational strain results in a distribution in g_i, on top of a distribution in D and E, which, as long as the regime $\nu \approx D$ is not reached, causes a severe broadening of the resonances, particularly at high magnetic fields. Hence, the absence of a spectrum at J band suggests that $|D|$ is larger than about 300 GHz.

If we compare the spin-Hamiltonian parameters of the active site of desulforedoxin to those of the active site of rubredoxin, we notice remarkable differences. First, the rhombicity of the ZFS-tensor of the high-spin Fe^{3+} sites differs considerably for desulforedoxin and rubredoxin. The D and λ of rubredoxin from *D. gigas* are known to be 48.5 GHz and 0.26,[5] while we find $D = 72$ GHz and $\lambda = 0.074$ for desulforedoxin. Second, while D is positive for the Fe^{3+} sites, D is negative for the

dx.doi.org/10.1021/jp3025655 | J. Phys. Chem. B 2012, 116, 7122−7128

Co(II)-substituted active site of desulforedoxin and, moreover, the rhombicity of Co(II)−desulforedoxin is comparable to that of the Fe^{3+} site of rubredoxin: $D < -300$ GHz and $\lambda = 0.26$. At this point it would be desirable to know the ZFS parameters of Co(II)-substituted rubredoxin,[49] but, unfortunately, we were not successful in obtaining an EPR spectrum of Co(II)−rubredoxin in spite of considerable effort.[50] However, the absence of an EPR spectrum suggests a $\lambda \approx 0$ and $D < 0$. In this situation a transition within the lowest doublet is (almost) forbidden and at elevated temperatures, where the higher doublet becomes populated, the transitions within this doublet may broaden strongly due to fast relaxation.

The electronic structure of sulfur-coordinated transition-metal sites is known to depend on the structure of the site beyond the first coordination sphere.[10−12,16,51] For both rubredoxin and desulforedoxin from *D. gigas* the structures are known to a high resolution.[8,52,53] The structure of Co(II)-substituted rubredoxin is indistinguishable from the structure of Fe(III)−rubredoxin by X-ray diffraction.[54] No X-ray diffraction study of the structure of Co(II)-substituted desulforedoxin has been performed, but we will assume that its structure is the same as that of Fe(III)−desulforedoxin.

Figure 6a shows the structure of the active site of rubredoxin. The $Fe(SC)_4$ geometry is approximately what is referred to in ref 12 as the $D_{2d}(1)$ or double-bird geometry. This conformation is the combined result of the site being built up from four cysteine residues on two amino acid strands and the sulfur-lone-pair repulsion. The FeS_4 core is elongated from T_d symmetry (two smaller angles and four larger ones).[51] Figure 6b shows the structure of the active site of desulforedoxin. The angle S−Fe−S involving Cys28 and Cys29 is relatively large, 121.5°, due to the adjacency of the two cysteines, and $C_9-S_9-Fe-S_{29}-C_{29}$ is not able to assume the bird geometry on the Cys29 side (the numbers of the C- and S atoms correspond to the number of the cysteine residue they are part of).

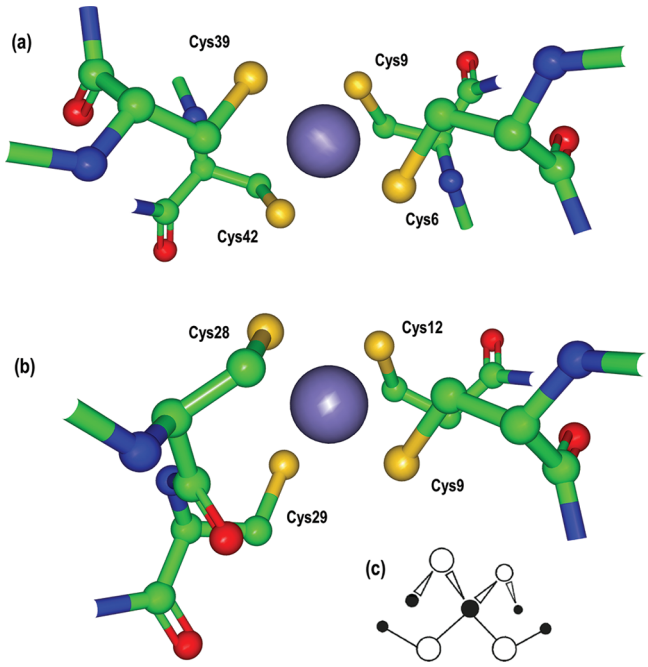

Figure 6. (a) Structure of the active site of rubredoxin from *D. gigas*. Color code for the elements: S, yellow; C, green; N, blue; O, red. (b) Structure of the active site of desulforedoxin from *D. gigas*. (c) Schematic drawing of the double-bird geometry.

Interpretation of the ZFS parameters in relation to the structure of the active sites is far from straightforward. Ligand-field considerations concerning the metal *d*-orbitals are of limited applicability because of the significant (anisotropic) covalency of the metal−sulfur bonds. Recently, the experimental ZFS parameters of a number of high-spin Co^{2+} complexes have been well reproduced by correlated ab initio calculations.[55] In particular, for the truncated double-bird core of the complex $[Co(SPh)_4]^{2-}$ a large negative D and $\lambda = 0$ were calculated, where $\lambda = 0$ already follows from the symmetry.[21] The approximate double-bird geometry of the rubredoxin active site suggests similar ZFS parameters for the high-spin Co^{2+} site, which would be in line with the ZFS parameters predicted from the absence of an EPR spectrum. In this respect the $\lambda = 0.26$ of the Co(II)-substituted active site of desulforedoxin, which is considerably more asymmetric than the rubredoxin site, is in line with expectations.

All interaction tensors must be axial if the symmetry of the site is D_{2d}. From this perspective the $\lambda = 0.26$ observed for high-spin Fe^{3+} rubredoxin is remarkable. Moreover, a ZFS tensor that is closer to axial, $\lambda = 0.074$, is observed for high-spin Fe^{3+} desulforedoxin. These observations illustrate how difficult it is to predict the effects of deviations from a presumed symmetry of a site on its electronic structure.

The deviations of symmetry in the sites of rubredoxin and desulforedoxin affect the electronic structure differently, depending on whether the site is occupied by high-spin Co^{2+} ($3d^7$ configuration) or high-spin Fe^{3+} ($3d^5$ configuration). These differences arise because the former has a ^4F ground state, while the latter has a ^6S ground state. The in-state orbital angular momentum of the high-spin Co^{2+} may be quenched by the low symmetry of the site, but is easily restored by mixing of the ground state with nearby excited states and a *g*-anisotropy and large ZFS are expected.[37] On the other hand, for high-spin Fe^{3+} no in-state orbital angular momentum and no ligand field excited states of the same multiplicity are present. The origin of the observed ZFS, which is much smaller than for high-spin Co^{2+}, lies mainly in anisotropy in the covalency, which even reverses the sign of D.[13,14,56]

CONCLUSION

High-frequency EPR spectroscopy provides valuable information on the electronic structure of high-spin transition-metal sites in biological systems. At the same time, the observation and analysis of the spectra is not straightforward, particularly in the case of high-spin Co^{2+}. Attempts to interpret the ZFS tensors and *g*-anisotropy observed for high-spin Fe^{3+} and high-spin Co^{2+} in the active sites of desulforedoxin and rubredoxin illustrate the necessity of further development of advanced quantum-chemical calculations, which can interrelate the geometric structure and electronic structure of these active sites.

AUTHOR INFORMATION

Corresponding Author

*E-mail: groenen@physics.leidenuniv.nl.

Notes

The authors declare no competing financial interest.

■ ACKNOWLEDGMENTS

The research was supported with financial aid by The Netherlands Organization for Scientific Research (NWO), Department of Chemical Sciences (CW).

■ REFERENCES

(1) Möbius, K.; Savitsky, A.; Schnegg, A.; Plato, M.; Fuchs, M. *Phys. Chem. Chem. Phys.* **2005**, *7*, 19−42.
(2) Solomon, E. I. *Inorg. Chem.* **2005**, *44*, 723−726.
(3) van Doorslaer, S.; Vinck, E. *Phys. Chem. Chem. Phys.* **2007**, *9*, 4620−4638.
(4) Kaupp, M.; Bühl, M.; Malkin, V. G. *Calculation of NMR and EPR Parameters*; Wiley-VCH Verlag GmbH & Co. KGaA: Weinheim, Germany, 2004.
(5) Mathies, G.; Blok, H.; Disselhorst, J. A. J. M.; Gast, P.; van der Meer, H.; Miedema, D. M.; Almeida, R. M.; Moura, J. J. G.; Hagen, W. R.; Groenen, E. J. J. *J. Magn. Reson.* **2011**, *210*, 126−132.
(6) Meyer, J.; Moulis, J.-M. *Handbook of Metalloproteins*; Wiley & Sons: New York, 2001; Chapter Rubredoxin, pp 505−517.
(7) Moura, I.; Bruschi, M.; Gall, J. L.; Moura, J. J. G.; Xavier, A. V. *Biochem. Biophys. Res. Commun.* **1977**, *75*, 1037−1044.
(8) Archer, M.; Huber, R.; Tavares, P.; Moura, I.; Moura, J. J. G.; Carrondo, M. A.; Sieker, L. C.; LeGall, J.; Romao, M. J. *J. Mol. Biol.* **1995**, *251*, 690−702.
(9) Bruschi, M.; Moura, I.; Gall, J. L.; Xavier, A. V.; Sierer, L. C.; Bovier-Lapierre, G.; Bonicel, J.; Couchoud, P. *Biochem. Biophys. Res. Commun.* **1979**, *90*, 596−605.
(10) Bair, R. A.; Goddard, W. A. *J. Am. Chem. Soc.* **1978**, *100*, 5669−5676.
(11) Ueyama, N.; Sugawara, T.; Tatsumi, K.; Nakamura, A. *Inorg. Chem.* **1987**, *26*, 1978−1981.
(12) Vrajmasu, V. V.; Münck, E.; Bominaar, E. L. *Inorg. Chem.* **2004**, *43*, 4867−4879.
(13) Deaton, J. C.; Gebhard, M. S.; Koch, S. A.; Millar, M.; Solomon, E. I. *J. Am. Chem. Soc.* **1988**, *110*, 6241−6243.
(14) Deaton, J. C.; Gebhard, M. S.; Solomon, E. I. *Inorg. Chem.* **1989**, *28*, 877−889.
(15) Gebhard, M. S.; Deaton, J. C.; Koch, S. A.; Millar, M.; Solomon, E. I. *J. Am. Chem. Soc.* **1990**, *112*, 2217−2231.
(16) Millar, M.; Lee, J. F.; O'Sullivan, T.; Koch, S. A.; Fikar, R. *Inorg. Chim. Acta* **1996**, *243*, 333−343.
(17) Peisach, J.; Blumberg, W. E.; Lode, E. T.; Coon, M. J. *J. Biol. Chem.* **1971**, *246*, 5877−5881.
(18) Moura, I.; Xavier, A. V.; Cammack, R.; Bruschi, M.; Gall, J. L. *Biochim. Biophys. Acta* **1978**, *533*, 156−162.
(19) Börger, B.; Suter, D. *J. Phys. Chem.* **2001**, *115*, 9821−9826.
(20) Fukui, K.; Ohya-Nishiguchi, H.; Hirota, N. *Bull. Chem. Soc. Jpn.* **1991**, *64*, 1205−1212.
(21) Fukui, K.; Kojima, N.; Ohya-Nishiguchi, H.; Hirota, N. *Inorg. Chem.* **1992**, *31*, 1338−1344.
(22) Fukui, K.; Masuda, H.; Ohya-Nishiguchi, H.; Kamada, H. *Inorg. Chim. Acta* **1995**, *238*, 73−81.
(23) Sottini, S.; Mathies, G.; Gast, P.; Maganas, D.; Kyritsis, P.; Groenen, E. J. J. *Phys. Chem. Chem. Phys.* **2009**, *11*, 6727−6732.
(24) Maganas, D.; Milikisyants, S.; Rijnbeek, J. M. A.; Sottini, S.; Levesanos, N.; Kyritsis, P.; Groenen, E. J. J. *Inorg. Chem.* **2010**, *49*, 595−605.
(25) Walsby, C. J.; Krepkiy, D.; Petering, D. H.; Hoffman, B. M. *J. Am. Chem. Soc.* **2003**, *125*, 7502−7503.
(26) Moura, I.; Huynh, B. H.; Hausinger, R. P.; Gall, J. L.; Xavier, A. V.; Münck, E. *J. Biol. Chem.* **1980**, *255*, 2493−2498.
(27) Yu, L.; Kennedy, M.; Czaja, C.; Tavares, P.; Moura, J. J. G.; Moura, I.; Rusnak, F. *Biochem. Biophys. Res. Commun.* **1997**, *231*, 679−682.
(28) Moura, I.; Teixeira, M.; LeGall, J.; Moura, J. J. G. *J. Inorg. Biochem.* **1991**, *44*, 127−139.
(29) Almeida, R. M.; Pauleta, S. R.; Moura, I.; Moura, J. J. G. *J. Inorg. Biochem.* **2009**, *103*, 1245−1253.
(30) Blok, H.; Disselhorst, J. A. J. M.; Orlinskii, S. B.; Schmidt, J. *J. Magn. Reson.* **2004**, *166*, 92−99.
(31) Disselhorst, J. A. J. M.; van der Meer, H.; Poluektov, O. G.; Schmidt, J. *J. Magn. Reson. Series A* **1995**, *115*, 183−188.
(32) Pardi, L. A.; Krzystek, J.; Telser, J.; Brunel, L.-C. *J. Magn. Reson.* **2000**, *146*, 375−378.
(33) Abragam, A.; Bleaney, B. *Electron Paramagnetic Resonance of Transition Ions*; Dover Publications: New York, 1986.
(34) Tavares, P.; Wunderlich, J. K.; Lloyd, S. G.; Gall, J. L.; Moura, J. J. G.; Moura, I. *Biochem. Biophys. Res. Commun.* **1995**, *208*, 680−687.
(35) Stoll, S.; Schweiger, A. *J. Magn. Reson.* **2006**, *178*, 42−55.
(36) Pilbrow, J. R. *J. Magn. Reson.* **1978**, *31*, 479−490.
(37) Banci, L.; Bencini, A.; Benelli, C.; Gatteschi, D.; Zanchini, C. *Struct. Bonding (Berlin)* **1982**, *52*, 37−86.
(38) Drulis, H.; Dyrek, K.; Hoffmann, K. P.; Hoffmann, S. K.; Weselucha-Birczynska, A. *Inorg. Chem.* **1985**, *24*, 4009−4012.
(39) Yang, A.-S.; Gaffney, B. J. *Biophys. J.* **1987**, *51*, 55−67.
(40) Barra, A.-L.; Gräslund, A.; Andersson, K. K. In *Biological Magnetic Resonance 22 - Very high frequency (VHF) ESR/EPR*; Grinberg, O. Y., Berliner, L. J., Eds.; Kluwer Academic/Plenum Publishers: Dordrecht, The Netherlands, 2004; Chapter 5. The use of very high frequency EPR (VHF-EPR) in studies of radicals and metal sites in proteins and small inorganic models, pp 145−163.
(41) Abragam, A.; Pryce, M. H. L. *Proc. R. Soc. London, Ser. A* **1951**, *205*, 135−153.
(42) Jesson, J. P. *J. Chem. Phys.* **1968**, *48*, 161−168.
(43) Pryce, M. H. L. *Proc. Phys. Soc., London, Sect. A* **1950**, *63*, 25−29.
(44) Bencini, A.; Gatteschi, D. *Inorg. Chem.* **1977**, *16*, 2141−2142.
(45) Beijers, H. G.; Bongers, P. F.; van Stapele, R. P.; Zijlstra, H. *Phys. Lett.* **1964**, *12*, 81−82.
(46) van Stapele, R. P.; Beijers, H. G.; Bongers, P. F.; Zijlstra, H. *J. Chem. Phys.* **1966**, *44*, 3719−3725.
(47) Krzystek, J.; Zvyagin, S. A.; Ozarowski, A.; Fiedler, A. T.; Brunold, T. C.; Telser, J. *J. Am. Chem. Soc.* **2004**, *126*, 2148−2155.
(48) Krzystek, J.; Swenson, D. C.; Zvyagin, S. A.; Smirnov, D.; Ozarowski, A.; Telser, J. *J. Am. Chem. Soc.* **2010**, *132*, 5241−5253.
(49) May, S. W.; Kuo, J.-Y. *Biochemistry* **1978**, *17*, 3333−3338.
(50) Mathies, G. Ph.D. Thesis *High-frequency EPR on high-spin transition-metal sites*; Leiden University: 2012.
(51) Vrajmasu, V. V.; Bominaar, E. L.; Meyer, J.; Münck, E. *Inorg. Chem.* **2002**, *41*, 6358−6371.
(52) Frey, M.; Sieker, L.; Payan, F.; Haser, R.; Bruschi, M.; Pepe, G.; LeGall, J. *J. Mol. Biol.* **1987**, *197*, 525−541.
(53) Chen, C.-J.; Lin, Y.-H.; Huang, Y.-C.; Liu, M.-Y. *Biochem. Biophys. Res. Commun.* **2006**, *349*, 79−90.
(54) Maher, M.; Cross, M.; Wilce, M. C. J.; Guss, J. M.; Wedd, A. G. *Acta Crys. Section D* **2004**, *60*, 298−303.
(55) Maganas, D.; Sottini, S.; Kyritsis, P.; Groenen, E. J. J.; Neese, F. *Inorg. Chem.* **2011**, *50*, 8741−8754.
(56) Solomon, E. I.; Brunold, T. C.; Davis, M. I.; Kemsley, J. N.; Lee, S.-K.; Lehnert, N.; Neese, F.; Skulan, A. J.; Yang, Y.-S.; Zhou, J. *Chem. Rev.* **2000**, *100*, 235−349.